Downregulation of ITIH3 contributes to cisplatin-based chemotherapy resistance in ovarian carcinoma via the Bcl-2 mediated anti-apoptosis signaling pathway

YINGZHAO LIU[1,2*], LIJUN SHI[3*], CUNZHONG YUAN[4,5], YAN FENG[6], MENGDI LI[2,6],
HONGMEI LIU[2,6], XI CHEN[2,6], DESHENG YAO[1,2] and QI WANG[2,6]

[1]Department of Gynecologic Oncology, Guangxi Medical University Affiliated Tumor Hospital; [2]Key Laboratory of Early
Prevention and Treatment for Regional High Frequency Tumor, Guangxi Medical University, Ministry of Education;
[3]Department of Oncology, The First Affiliated Hospital of Guangxi Medical University, Nanning, Guangxi Zhuang
Autonomous Region 530021; [4]Department of Obstetrics and Gynecology; [5]Gynecology Oncology Key Laboratory,
Qilu Hospital of Shandong University, Jinan, Shandong 250012; [6]Research Department, Guangxi Medical
University Affiliated Tumor Hospital, Nanning, Guangxi Zhuang Autonomous Region 530021, P.R. China

Abstract. Platinum resistance of ovarian cancer is one of the primary factors of poor prognosis and inter-α-trypsin inhibitor heavy chain 3 (ITIH3) is a potential DDP resistance-associated gene. The present study assessed protein expression levels of ITIH3 in human ovarian cancer and evaluated the relationship between its expression and platinum-resistance in patients. Furthermore, the effect of ITIH3 on cisplatin (DDP)-resistant ovarian cancer cells and the underlying molecular mechanism were evaluated. Tissue microarrays of ovarian cancer samples were used to assess the association between ITIH3 protein expression levels and drug resistance and the prognosis of ovarian cancer. ITIH3 RNA interference (RNAi) ovarian cancer cell lines were constructed and expression levels of anti- and pro-apoptotic proteins of the Bcl-2 associated pathway, including Bcl-2, Bcl-xL, Mcl-1, Bak, Bim, Bax, caspase 3 and poly ADP-ribose polymerase (PARP), were assessed following DDP treatment. The Bcl-2 inhibitor ABT-737 was used to rescue DDP-resistance induced by loss of ITIH3 *in vitro*. Finally, a subcutaneous xenograft tumor model was used to evaluate the effect of multiple DDP injections on expression levels of apoptosis-related proteins

like Bcl-2, Bcl-xL, Bak, caspase 3 and PARP. The results of tissue microarray immunohistochemistry revealed that decreased ITIH3 protein expression levels were associated with a shorter overall survival for patients with ovarian cancer. The results of Cell Counting Kit-8 assay showed that the half-maximal inhibitory concentration and resistance index of DDP in SKOV3-ITIH3 and OVCAR3-ITIH3 RNAi cells were significantly higher than in control groups. Following DDP treatment, the results of western blotting revealed that expression levels of anti-apoptotic proteins of the Bcl-2 family significantly increased in SKOV3-ITIH3 and OVCAR3-ITIH3 RNAi cells. Pro-apoptotic protein expression was not significantly changed following DDP treatment, whereas cleaved caspase 3, caspase 3 and cleaved (C-PARP) were markedly downregulated. The Bcl-2 inhibitor ABT-737 was demonstrated to reverse increased DDP resistance induced by ITIH3 expression in flow cytometric and western blotting analysis. In the subcutaneous murine xenograft model, an increased number of DDP injections yielded a decrease in phosphorylated Bcl-2, cleaved caspase 3, caspase 3 and C-PARP protein expression levels in the SKOV3-ITIH3 RNAi group tested by western blotting. To the best of our knowledge, this is the first study to demonstrate that ITIH3 could be a vital molecule involved in chemosensitivity via regulation of the Bcl-2 family-mediated apoptotic pathway. Lower protein expression levels of ITIH3 were significantly associated with platinum resistance and poor prognosis in ovarian cancer. ITIH3 may predict cisplatin-resistance in ovarian cancer.

Correspondence to: Professor Qi Wang or Professor Desheng Yao, Key Laboratory of Early Prevention and Treatment for Regional High Frequency Tumor, Guangxi Medical University, Ministry of Education, 22 Shuangyong Road, Nanning, Guangxi Zhuang Autonomous Region 530021, P.R. China
E-mail: wangqi@stu.gxmu.edu.cn
E-mail: yaodeson@163.com

*Contributed equally

Introduction

Ovarian cancer (OC) has the highest mortality rate of gynecological cancer (1). Since cisplatin (DDP) was approved by Food and Drug Administration (USA) in 1978, platinum anticancer drugs have become the most widely used type of chemotherapy drug (2). Platinum/taxane-based chemotherapy is currently the first-line treatment for OC. Patients often initially

respond well to platinum-based chemotherapy combined with paclitaxel administration. However, a marked proportion of patients experience disease recurrence. Furthermore, resistance to platinum-based chemotherapy is correlated with poor prognosis (3). Once patients with OC present with recurrence and/or chemotherapeutic resistance, the median overall survival (OS) is only 12-14 months (3). Tumor resistance to platinum drugs is reportedly one of the primary factors that limits the efficacy of OC treatment (4). Accordingly, research on platinum resistance is essential to improve the survival of this patient population.

In a previous study, an *in vivo* model of platinum-resistant OC was established by simulating the clinical drug resistance process (5). Through study of the mouse model, it was demonstrated that inter-α-trypsin inhibitor heavy chain 3 (ITIH3) was downregulated in the platinum-resistant OC group. It was hypothesized that ITIH3 may be a DDP resistance-associated gene. The ITIH3 gene encodes the heavy chain subunit of the α trypsin inhibitor complex precursor that stabilizes the extracellular matrix by preventing hyaluronic acid depolymerization (6,7). ITIH3 may also serve an important role in tumor progression. There is ample evidence to suggest that the ITIH family genes are markedly downregulated in various human solid tumors, such as colon, breast and lung cancer, which indicates that the ITIH family may be tumor suppressor genes (8,9). Abnormally elevated blood ITIH3 expression levels have been reported in patients with pancreatic (10,11), early gastric (12), breast (13) and colorectal cancer (9). Furthermore, ITIH3 has been reported to be abnormally elevated in the serum of mouse models of gastric and colorectal cancer (12,14). Taken together, these findings suggest that ITIH3 has potential as a tumor marker. To the best of our knowledge, however, few studies have reported the role of ITIH3 expression in OC (13,15). One study reported that ITIH3 mRNA expression levels are significantly downregulated in 71% of OC cases, which indicated that ITIH3 may be a tumor suppressor gene (8). To the best of our knowledge, there are no published reports about the connection between ITIH3 and DDP resistance. Therefore, in the present study the effect of ITIH3 expression on platinum resistance in OC was assessed and the association between ITIH3 expression levels and survival were evaluated. *In vivo* and *in vitro* experiments were used to investigate the underlying mechanism of action.

Materials and methods

Patient information. OC tumor tissue microarrays (TMAs) were gifted from Professor Beihua Kong (Qilu Hospital of Shandong University, Jinan, China). The present study was approved by the Scientific Ethics Committee of Qilu Hospital of Shandong University (approval no. KYLL-2013-130). All participants provided written informed consent for the present study.

TMAs were obtained for late-stage OC tissue specimens (n=109) collected from January 2005-December 2013 at Qilu Hospital of Shangdong University (Table I). TMA analysis was performed as described previously (16). Patients were followed-up every month for the first year after surgery, every 3 months for the second year, every 6 months for the third year and once/3 years thereafter. OS was defined as the time from

Table I. Pathological features of 109 patients with epithelial ovarian cancer.

Pathological feature	Cases	ITIH3 IRS	P-value
Vital status			0.04
Living	37	6.22±2.66	
Deceased	72	5.11±2.50	
FIGO			0.33
Stage III	100	5.56±2.65	
Stage IV	9	4.67±1.94	
Pathological grade			
G2-3	109	5.49±2.60	
Histological classification			0.88
Serous	103	5.50±2.63	
Non-serous	6	5.33±2.06	
Mucinous	1	8.00±0.00	
Endometrioid	2	4.00±0.00	
Mixed	3	5.33±2.31	

IRS, immunoreactive score; ITIH3, inter-α-trypsin inhibitor heavy chain 3; FIGO, International Federation of Gynecology and Obstetrics.

the day of diagnosis to death. The follow-up period ranged from 0.6-129.0 months (mean, 41.5±25.9 months). Progression-free survival (PFS) was defined as the period from the day of surgery to the time of disease recurrence. Data of patients who did not experience disease recurrence and survived beyond April 1, 2016, are recorded as censored data.

Cell culture. The OC SKOV3 cell line was gifted from Professor Hani Gabra (Imperial College London, London, UK) and a DDP-resistant cell line SKOV3/DDPII was developed in the laboratory as previously described (5). The OC A2780 and CAOV3 cell lines were purchased from the National Infrastructure of Cell Line Resource. The OC NIH:OVCAR3 cell line was purchased from the American Type Culture Collection. SKOV3, SKOV3/DDPII and CAOV3 cells were cultured at 37˚C under 5% CO_2 in Dulbecco's modified Eagle medium/high glucose medium (DMEM; Corning, Inc.) supplemented with 10% fetal bovine serum (Corning, Inc.), 100 IU/ml penicillin and 100 IU/ml streptomycin. A2780 cells were cultured at 37˚C under 5% CO_2 in RPMI-1640 (Corning, Inc.) supplemented with 10% fetal bovine serum (Corning), 100 IU/ml penicillin and 100 IU/ml streptomycin. OVCAR3 cells were cultured at 37˚C under 5% CO_2 in RPMI-1640 complete medium (Shanghai Yingwan Biological Co., Ltd.).

Immunohistochemistry. Immunohistochemistry of TMAs was performed on 4 μm sections sliced from each TMA receiver block fixed with 4% paraformaldehyde at room temperature for 48 h and embedded in paraffin. The production of TMAs was performed as described previously (17,18). ITIH3 protein expression levels were assessed using an Immunohistochemistry Envision Horseradish Peroxidase kit

(cat. no. KIT-5004; Fuzhou Maixin Biotech. Co., Ltd.) and goat-antiITI-H3 (L-15) antibody (1:200; cat. no. sc-33949; Santa Cruz Biotechnology, Inc.). At room temperature, sections were incubated with primary antibody for 1 h. The sections were next incubated with secondary anti-goat (1:500; cat. no. P0449; Dako, Agilent Technologies, Inc.) antibodies for 20 min at RT. Two senior pathologists who were blinded to the research independently evaluated and scored the proportion of positively stained cells in each specimen and staining intensity under microscope (Olympus, Inc.). The proportion of positive cells was scored as follows: 0, no positive cells; 1, 1-25; 2, 26-50; 3, 51-75 and 4, 76-100% positive cells. Staining intensity was scored as follows: 0, no color; 1, pale yellow; 2, brown and 3, dark brown. The final immunoreactive score (IRS) was the product of the positive cell proportion score and the staining intensity score. For ITIH3, a final IRS of 0 was defined as negative, ≤6 as weak expression and >6 as strong expression (19).

Construction of ITIH3 RNA interference (i) cell lines. Lentiviruses expressing ITIH3 short hairpin (sh)RNA were produced using 0.5 μg Lentiviral shRNA Vectors LV-3 (pGLVH1/GFP + Puro), which targeted the sequence 5'-GCA ACGTGCAGATAGTCA ATG-3', combined with 1.5 μg third-generation lentiviral packaging mix (1:1:1 mix of PG-P1-VSVG, PG-P2-REV and PG-P3-RRE) in 293T cells. Lentiviruses expressing nonsense sequence shRNA were used as the negative control (NC) (5'-GTTCTCCGA ACG TGTCACGT-3'). Lentiviruses were purchased from Suzhou GenePharma Co., Ltd. SKOV3 cells were plated in 6-well plates at a density of $1x10^5$ cells/well in 1 ml DMEM (Corning, Inc.). The cells were treated with virus venom (MOI=5-10) and polybrene solution (5 μg/ml) at a cell saturation of ~30% at 37°C for 24 h. After 24 h, the medium was replaced with fresh culture medium and cells were cultured at 37°C. After 72 h of transduction, cells were screened using GFP fluorescence and selected by 2-5 μg/ml puromycin (cat. no. ant-pr-1; InvivoGen, Inc.) for 5-7 days.

The ITIIH3 small interfering (si)RNA oligo (5'-GCAUCA GUAUGCUGA ACAATT-3') and a scrambled non-targeting siRNA (siNC; 5'-UUCUCCGA ACGUGUCACGUTT-3') were purchased from Suzhou GenePharma Co., Ltd. OVCAR3 cells at 70% confluency were transfected with a final concentration of 10 nM siITIH3 or siNC at 37°C for 24 h using HiPerFect® Transfection Reagent (Qiagen GmbH) according to the manufacturer's protocol. After 72 h, western blotting using ITIH3 antibody was performed to assess depletion efficiency.

Cytotoxicity assay. The half-maximal inhibitory concentration (IC$_{50}$) of DDP was assessed using Cell Counting Kit-8 (CCK-8; Dojindo Laboratories, Inc.) assay. SKOV3, SKOV3-NC, SKOV3-ITIH3 RNAi, SKOV3/DDPII, OVCAR3, OVCAR3-NC or OVCAR3-ITIH3 RNAi cells were cultured in a medium containing a DDP gradient (1.25, 2.50, 5.00, 10.00 and 20.00 μM) at 37°C for 48 h. CCK8 reagent (10 μl) was added to each well, followed by incubation for 2 h at 37°C. The absorbance was assessed at 450 nm. Cell proliferation inhibition at different drug concentrations was calculated as follows: Inhibition rate=(control well absorbance-test well absorbance)/(control well absorbance-blank well absorbance) (20).

Five replicate wells were used/concentration and the experiment was repeated at least three times. The IC$_{50}$ value and DDP resistance at 48 h were calculated using SPSS 20.0 (IBM Corp.). And the drug resistance index=IC$_{50}$ of drug-resistant cells/IC$_{50}$ of parental cells.

Cell viability and cytotoxicity assay. Cell viability and drug toxicity analyses were performed using a real-time cell analysis (RTCA) xCELLigence D.P. system (ACEA Bioscience, Inc.), a real-time label-free system used to monitor cell viability, migration and invasion. SKOV3-NC or SKOV3-ITIH3 RNAi cells were plated in a 16-well culture plate and incubated overnight in DMEM supplemented with 10% fetal bovine serum (Corning, Inc.) for toxicity analysis. Cells in the exponential growth phase were treated using DDP (10 or 20 μM) at 37°C for 100 h. The cell viability and proliferation were assessed every 15 min for 100 h. Duplicate wells were used for each concentration. The results were presented as the normalized cell index (CI), which was derived from the CI ratio before and after drug treatment by RTCA 2.0.0.1301 software (ACEA Bioscience, Inc.).

Colony formation assay. SKOV3, SKOV3-NC, SKOV3-ITIH3 RNAi or SKOV3/DDPII cells were plated at a density of 1,000 cells/well in 6-well plates and incubated in DMEM supplemented with 10% fetal bovine serum (Corning, Inc.) at 37°C overnight. Then, 0.3 or 0.6 μM DDP was added, followed by incubation at 37°C for 2 days. The culture media was replaced and cells were cultured at 37°C for another 5 days. Colonies were fixed using 100% cold methanol for 15 min in 4°C and stained using 10% Giemsa's Stain (cat. no. G8220; Beijing Solarbio Science & Technology Co., Inc.) for 30 min in RT. The stained colonies were visualized using a light microscope (magnification, x40) (Nikon, Inc.) and the number of colonies that contained >50 cells were counted manually. Experiments were repeated three times and three parallel wells were used/concentration.

Flow cytometric analysis of apoptosis. Apoptosis of SKOV3, SKOV3-NC, SKOV3-ITIH3 RNAi or SKOV3/DDPII cells was assessed using flow cytometry using a PE Annexin V Apoptosis Detection kit I assay (BD Biosciences), according to the manufacturer's protocols. Each sample was assessed using a CytoFLEX flow cytometer (Beckman Coulter, Inc.). The results were quantified using CytExpert 2.1.0.92 (Beckman Coulter, Inc.). The apoptotic rate was calculated as the sum of early apoptosis rate (first quadrant) and the late apoptosis rate (fourth quadrant). All experiments were repeated at least three times.

Xenograft modelling. In our previously study, we developed a DDP-resistant cell line with stable DDP resistance index and platinum resistant epithelial ovarian cancer mice mode1, the specific methods were performed as described previously (5). Briefly, subcutaneous xenograft tumor models of SKOV3 and SKOV3/DDPII were established in nude mice. When all tumor volume reached >400 mm^3, 2.5 mg/kg DDP was administered by intraperitoneal injection every other day for a maximum of eight doses. Tumors were removed on before injection (0 does) and 2 days following the 2, 5 and 8 times (2, 5 and 8 does)

of DDP injections. The removed tumors were immediately frozen in liquid nitrogen for follow-up proteomic studies.

Isobaric tag for relative and absolute quantitation (iTRAQ) proteomics profiling. Subcellular membrane, nuclear and cytoplasmic protein was extracted from xenograft tumors using the ProteoExtract Subcellular Proteome Extraction kit (539790; Merck KGaA) and mixed quantified using the Pierce BCA Protein Assay kit (23227; Thermo Fisher Scientific, Inc.). Protein samples were quantified, alkylated, digested and labeled with iTRAQ using the iTraq Reagent 8 plex buffer kit (4381663; Applied Biosystems; Thermo Fisher Scientific, Inc.) and iTraq Reagent 8 plex Multiplex kit (4381663; Applied Biosystems; Thermo Fisher Scientific, Inc.) according to the manufacturer's protocol. Following iTRAQ labeling, samples (100 μg/sample) were fractionated used a ACQUITY Ultra Performance LC system (Waters). The labeled samples were fractionated by strong cation exchange liquid chromatograph (SCX) using a 0.5x23.00 mm, 5 μm, 300A Column (Waters, USA). Second, ten fractions that eluted with 10 different molar concentration of 25, 50, 75, 100, 150, 200, 300, 400, 500 and 1,000 mM of NH4AC were collected from the SCX column. Then, each of the fractions was then loaded onto a reverse phase (RP) column, ZORBAX 300SB-C18 column (5 μm, 300A, 4.6x50.00 mm, Agilent, USA), both Buffer A (5% acetonitrile, 95% water, 0.1% formic acid) and Buffer B (95% acetonitrile, 5% water, 0.1% formic acid) were used for elution at a flow rate of 0.4 μl/min. The entire process was monitored at 214 nm absorbance at RT. The liquid chromatography eluent was assessed using high-resolution liquid chromatography with tandem mass spectrometry using a QStar Pulsar Quadrupole Time of Flight mass spectrometer (Applied Biosystems; Thermo Fisher Scientific, Inc.). ProteinPilot (2.0.1; Applied Biosystems; Thermo Fisher Scientific, Inc.) was used for protein identification and quantification after searching against the human International Protein Index database (IPI version 3.28, European Bioinformatics Institute, ebi.ac.uk/IPI), as previously described (21). The difference in protein expression levels was evaluated as described previously (16).

Western blotting. Total protein extracts of cells or mice xenograft tumor tissue were obtained using radioimmunoprecipitation assay lysis buffer (cat. no. R0010; Beijing Solarbio Science & Technology Co., Ltd.). Protein concentration was quantified using the Pierce BCA Protein Assay kit (23227; Thermo Fisher Scientific, Inc.). An equal amount of 40-60 μg protein from each sample was separated via 10-12% SDS-PAGE and transferred onto polyvinylidene fluoride membranes (MilliporeSigma) at 200 mA for 2 h on ice. The membranes were blocked in 5% non-fat milk (cat. no. LP0033; Thermo Fisher Oxoid, Inc.) at 4˚C for 2 h followed by incubation overnight with primary antibodies against different proteins at 4˚C. Western blotting was performed using the following primary antibodies: Bcl-2 (D55G8) Rabbit mAb (1:1,000; cat. no. 4223), Bcl-xL (54H6) Rabbit mAb (1:1,000; cat. no. 2764), Mcl-1 (D35A5) Rabbit mAb (1:1,000; cat. no. 5453), Phospho-Bcl-2 (Thr56) Antibody (1:1,000; cat. no. 2875), Phospho-Bcl-2 (Ser70; 5H2) Rabbit mAb (1:1,000; cat. no. 2827), Bak (D4E4) Rabbit mAb (1:1,000; cat. no. 12105), Bim (C34C5) Rabbit mAb (1:1,000; cat. no. 2933), Bax (D2E11) Rabbit

mAb (1:1,000; cat. no. 5023), Caspase-3 (8G10) Rabbit mAb (1:1,000; cat. no. 9665), poly ADP-ribose polymerase PARP antibody (1:1,000; cat. no. 9542), Cleaved PARP (Asp214; D64E10) XP® Rabbit mAb (1:1,000; cat. no. 5625), α-tubulin antibody (1:3,000; cat. no. 3873S) and rabbit anti-actin antibody (1:3,000; cat. no. 4970S), all purchased from Cell Signaling Technology, Inc. Bcl-2 Rabbit mAb (1:1,000; cat. no. R22494) was purchased from Chengdu Zhengneng Biotechnology Co., Ltd. and ITIH3 (1:1,000; cat. no. sc-33949) antibodies was purchased from Santa Cruz Biotechnology Co., Ltd. Cleaved caspase-3 (1:1,000; cat. no. ab32042) and rabbit anti-GAPDH (1:3,000; cat. no. ab181602) was purchased from Abcam. After washing with tris-buffered saline with 0.1% Tween-20, the membranes were probed with secondary antibodies at 4˚C for 2 h. The secondary anti-mouse (1:3,000; cat. no. 7076P2) and anti-rabbit (1:3,000; cat. no. 7074P2) antibodies were purchased from Cell Signaling Technology, Inc. and anti-goat (1:1,000; cat. no. P0449) antibodies were purchased from Dako (Agilent Technologies, Inc.). The immunoreactive bands were visualized using Pierce® ECL Western Blotting Substrate (cat. no. 32106; Thermo Fisher Scientific, Inc.), SuperSignal West Pico PLUS Chemiluminescent Substrate (cat. no. 34580; Thermo Fisher Scientific, Inc.) and the Fluor Chem M System (ProteinSimple). All experiments were repeated at least three times. The results were semi-quantified using AlphaView® 3.4.0 software (AlphaView SA) and band density was normalized to the corresponding loading control. The expression levels of phosphorylated proteins were presented as the ratio of phosphorylated to total protein.

Animal experiments. BALB/c nude female mice (n=40; age, 4 weeks; weight, 18-20 g) were purchased from and maintained under specific-pathogen-free (SPF) conditions at the Guangxi Medical University Laboratory Animal Center. A total of five mice were housed/cage under a 12/12-h light/dark cycle at 23±2˚C with 40-70% humidity. All mice had free access to SPF grade water and food. The mice were adapted to these conditions for at least 7 days prior to the experiments. All animal experiments were approved by the Animal Ethics Committee of Guangxi Medical University Affiliated Tumor Hospital (approval no. 2021057). The animal study was performed in compliance with the Animal Research: Reporting of *In Vivo* Experiments guidelines (22).

A total of 1x10^6 SKOV3-NC or SKOV3-ITIH3 RNAi cells were subcutaneously injected into the groin of nude mice (n=20 per cell line). The longest and shortest diameters of tumors were assessed using a Vernier caliper every three days before DDP injection and every other day following DDP injection; tumor volume was calculated as follows: Tumor volume=(length x width^2)/2. When all tumor volume reached >400 mm^3, the mice were randomly divided into four DDP injection groups (0, 2, 5 and 8 doses), with each group containing 5 mice. For the 0 DDP group, tumor tissue was removed before DDP injection. A total of 2.5 mg/kg DDP was administered by intraperitoneal injection every other day for a maximum of eight doses, according to the group, as previously described (5). Tumors were removed on 2 days following the last intraperitoneal injection of DDP in each group. At the end of the study, mice were euthanized by cervical dislocation under 2% isoflurane inhalation anesthesia and tumors were

removed and immediately frozen in liquid nitrogen. Death was confirmed when the mice stopped breathing and had no heartbeat. Humane endpoints were as follows: Total volume of a single tumor >1,500 mm^3 or 20% body weight loss. No animals reached these humane endpoints.

Statistical analysis. SPSS for Windows (version 20.0; IBM Corp) was used for all statistical analysis. Data of three repeated experiments are presented as the mean ± standard deviation. Comparisons between groups were assessed using one-way analysis of variance and Dunnett's post hoc test. Kaplan-Meier analysis with the log-rank (Mantel-Cox) comparison test was used to estimate the survival curves of different groups. P<0.05 was considered to indicate a statistically significant difference.

Results

Lower expression of ITIH3 is associated with DDP resistance in OC. In a preliminary study, an *in vivo* model of platinum-resistant OC was established and a drug-resistant cell line (SKOV3/DDPII) with a stable DDP resistance index was developed (5). A subcutaneous murine xenograft model using SKOV3 cells and SKOV3/DDPII cells treated with DDP was established (Fig. 1A). Tumor tissue collected after 0, 2, 5 or 8 injections of DDP were assessed using iTRAQ proteomics profiling and western blotting. iTRAQ proteomics profiling results demonstrated that protein expression levels of ITIH3 in subcutaneous xenograft tumors of the DDP-resistant group (SKOV3/DDPII group) after 0, 2, 5 or 8 DDP injections were markedly lower compared with those in the control SKOV3 group (Fig. 1B). Two iTRAQ replicates were performed to ensure the consistency and reliability of the results. Western blotting in the subcutaneous xenograft tumor demonstrated that ITIH3 protein expression levels in the SKOV3/DDPII group without DDP injection were significantly lower compared with those in the SKOV3 group (Fig. 1C). ITIH3 protein expression levels in the SKOV3/DDPII group were significantly lower than those in the SKOV3 group for all numbers of DDP doses.

Loss of ITIH3 protein expression is associated with poor prognosis in patients with OC. Of 109 patients with late-stage OC, 72 died during the follow-up period. The mean time of death was 31.08 months after surgery and the mean OS time was 41.46 months. An immunohistochemistry assay was used to assess ITIH3 protein expression levels in patient tumor tissue. The product of the proportion of positive cells and staining intensity scores was used to divide cells into high and low expression groups based on the final IRS, the cut-off value was set to 6 (IRS ≤6, low expression; IRS >6, high expression) (Fig. 1D). The ITIH3 IRS of patients who survived to the end of the study period was significantly higher than that of patients who died (Table I). The high ITIH3 protein expression level group demonstrated significantly higher OS compared with the low expression group (Fig. 1E). However, the difference was not significant with respect to the progression-free survival (Fig. 1F).

Establishment and validation of the ITIH3 RNAi cell lines. ITIH3 protein expression levels of four human OC cell lines (SKOV3, A2780, OVCAR3 and CAOV3) were assessed using western blotting. SKOV3 and OVCAR3 demonstrated markedly higher ITIH3 protein expression levels (Fig. 2A), therefore these lines were used in the RNAi experiments.

The SKOV3-ITIH3 RNAi cell line was constructed and cell fluorescence rate was >80% (data not shown). ITIH3 protein expression levels in SKOV3-ITIH3 RNAi cells were ~30% of those in the parent SKOV3 and SKOV3-NC cells (Fig. 2B), which was similar to ITIH3 protein expression levels in drug-resistant SKOV3/DDPII cells *in vitro*. An OVCAR3-ITIH3 RNAi cell line was constructed and the protein expression levels of ITIH3 were ~18% of those in the parent OVCAR3 cell line (Fig. 2C).

ITIH3 silencing increases DDP resistance in OC cells. CCK-8 assay demonstrated that the DDP IC$_{50}$ in SKOV3-ITIH3 RNAi cells was significantly higher compared with that in the parent SKOV3 and SKOV3-NC cells (P<0.001). The drug resistance index was ~2.08 times higher in SKOV3-ITIH3 RNAi cells than in SKOV3 cells (Fig. 2D) and close to the drug resistance index of SKOV3/DDPII cells. Furthermore, the DDP IC$_{50}$ in OVCAR3-ITIH3 RNAi cells after 48 h DDP treatment was significantly higher than that in the control OVCAR3 and OVCAR3-NC cells (Fig. 2E).

The dynamic changes in SKOV3-ITIH3 RNAi and SKOV3-NC cells treated with 10 or 20 μM DDP were assessed using the xCELLigence RTCA system. The normalized CI curve of SKOV3-ITIH3 RNAi cells at each DDP concentration was markedly higher than that of SKOV3-NC cells, which indicated higher proliferation in SKOV3-ITIH3 RNAi than in SKOV3-NC cells treated with DDP (Fig. 2F). Following treatment with 10 μM DDP, the normalized CI value of SKOV3-NC cells decreased to 0 at 80 h; however, the normalized CI value of SKOV3-ITIH3 RNAi cells decreased by ~50% and exhibited a tendency to increase again. The normalized CI value of SKOV3-ITIH3 RNAi cells was markedly higher than that of SKOV3-NC cells after DDP treated.

Silencing of ITIH3 attenuates colony formation of SKOV3 cells under DDP pressure. During the colony formation experiment, no significant difference between the number of SKOV3, SKOV3-NC, SKOV3-ITIH3 RNAi or SKOV3-DDPII cells was observed at any time point without drug treatment (Fig. 2G). Following DDP treatment (0.3 or 0.6 μM), the number of SKOV3-ITIH3 RNAi cells was significantly higher compared with the number of SKOV3 and SKOV3-NC cells, which was consistent with the number of colonies formed by SKOV3/DDPII cells *in vitro*.

ITIH3 silencing decreases DDP-induced apoptosis of SKOV3 cells. Flow cytometry demonstrated no significant difference in the proportion of apoptotic SKOV3, SkOV3-NC, SkOV3-ITIH3 RNAi and SKOV3-DDPII cells without drug treatment (Fig. 2H). However, following DDP (20 μM) treatment, the proportion of apoptotic SKOV3-ITIH3 RNAi cells was significantly lower than the proportion of apoptotic SKOV3 and SKOV3-NC cells at 72 h and slightly higher than the proportion of apoptotic DDP-resistant SKOV3/DDPII cells.

ITIH3 may be an upstream regulator of Bcl-2 signaling that promotes apoptosis induced by DDP in vitro. Bcl-2 family
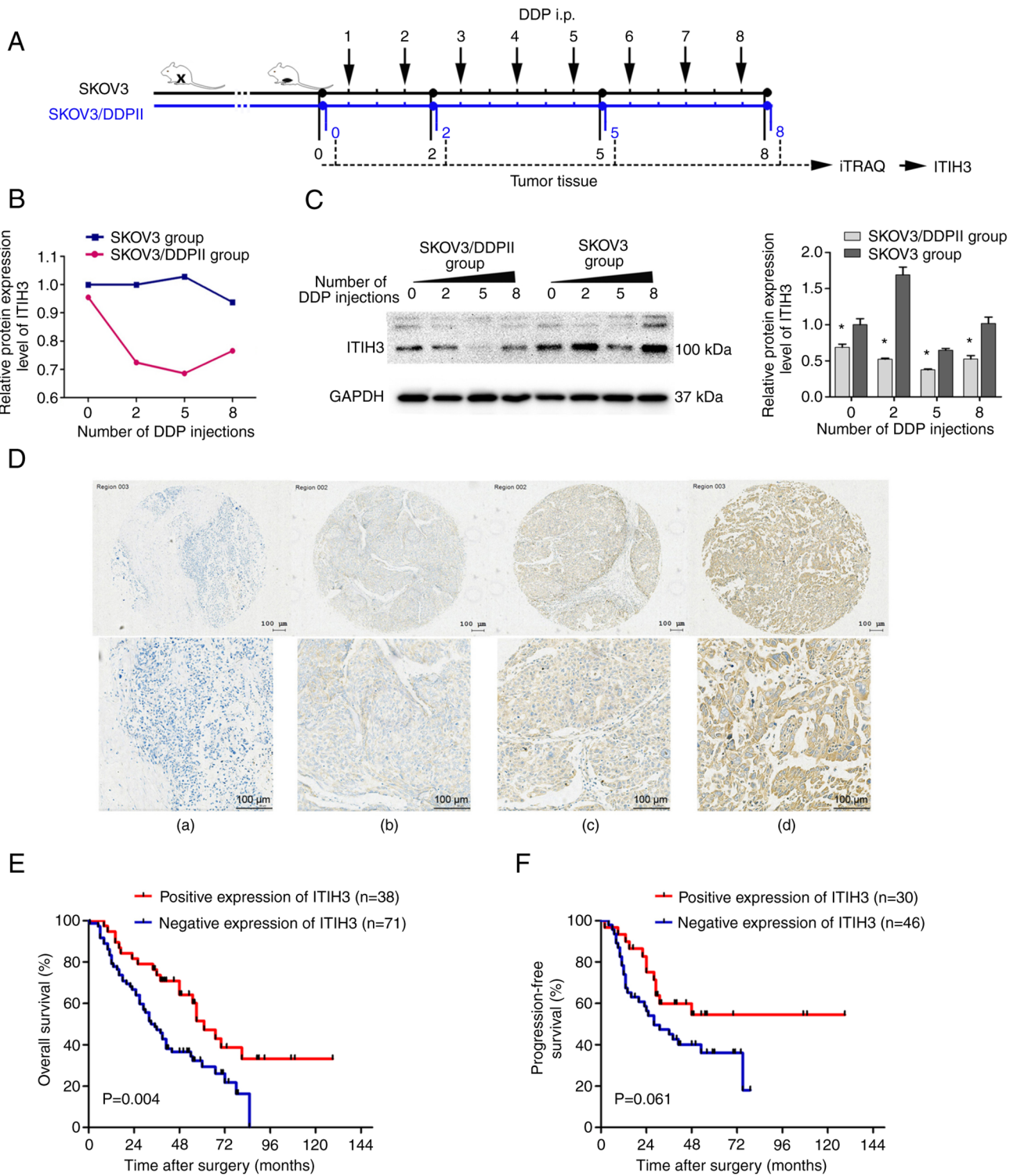
Figure 1. Lower protein expression levels of ITIH3 are associated with DDP resistance in OC. (A) Experimental design of the mouse study. (B) iTRAQ proteomics profiling of ITIH3 protein expression levels in SKOV3/DDPII- and SKOV3-derived subcutaneous tumor xenografts in nude mice after 0, 2, 5 and 8 DDP injections (2.5 mg/kg). A total of two iTRAQ replicates were performed. (C) Western blotting of the ITIH3 protein expression levels in SKOV3/DDPII- and SKOV3-derived subcutaneous tumor xenografts in nude mice following 0, 2, 5 and 8 DDP injections (2.5 mg/kg). GAPDH was used as a loading control. (D) Typical tissue microarray samples with (a) no color, (b) pale yellow, (c) brown and (d) dark brown color, evaluated using immunohistochemistry. Kaplan-Meier (E) overall and (F) progression-free survival analysis of high and low (cut-off=6) ITIH3 protein expression groups in patients with OC. *P<0.05 vs. SKOV3 group. ITIH3, inter-α-trypsin inhibitor heavy chain 3; iTRAQ, isobaric tag for relative and absolute quantitation; DDP, cisplatin; OC, ovarian cancer; i.p., intraperitoneal.

proteins, including pro-survival and pro-apoptotic proteins, serve key roles in apoptosis (Fig. 3A). Before DDP treatment, expression levels of Bcl-2 family proteins demonstrated no significant differences in SKOV3, SKOV3-NC, SKOV3-ITIH3 RNAi and SKOV3-DDPII cells (Fig. 3B). Following treatment with 10 μM DDP for 12, 24, 36 and 48 h, expression
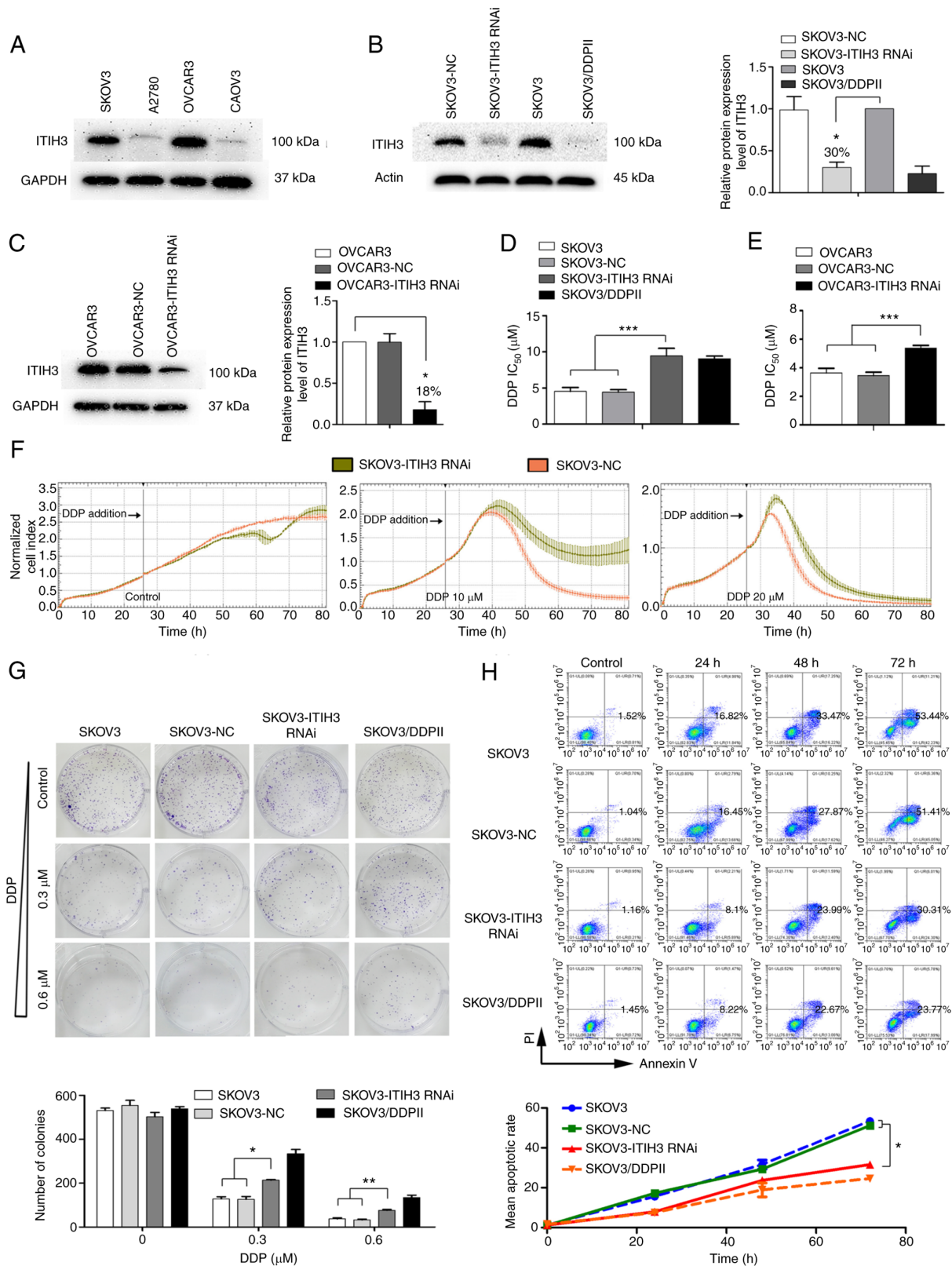
Figure 2. ITIH3 silencing in SKOV3 cells enhances DDP resistance. (A) Western blotting was used to assess ITIH3 protein expression levels in SKOV3, A2780, OVCAR3 and CAOV3 cells. GAPDH was used as a loading control. (B) Western blotting was used to assess ITIH3 protein expression levels (relative to SKOV3) in SKOV3-NC, SKOV3-ITIH3 RNAi, SKOV3 and SKOV3/DDPII cells. Actin was used as a loading control. (C) Western blotting was used to assess ITIH3 protein expression levels (relative to OVCAR3) in OVCAR3, OVCAR3-NC and OVCAR3-ITIH3 RNAi cells. GAPDH was used as a loading control. (D) IC_{50} of SKOV3, SKOV3-NC, SKOV3-ITIH3 RNAi and SKOV3/DDPII cells following 48 h DDP treatment. (E) IC50 of OVCAR3, OVCAR3-NC and OVCAR3-ITIH3 RNAi cells following 48 h DDP treatment. (F) Real-time analysis of the cytotoxic effect of DDP in SKOV3-ITIH3 RNAi and SKOV3-NC cells. (G) Colony formation experiments were performed using SKOV3, SKOV3-NC, SKOV3-ITIH3 RNAi and SKOV3/DDPII cell lines to assess the effects of ITIH3 on cell proliferation. Histograms display the mean number of colonies. (H) SKOV3-ITIH3 RNAi, control SKOV3, SKOV3-NC and positive control SKOV3/DDPII cells were treated with 20 μM DDP for 24, 48 and 72 h. Apoptotic cell death was assessed using Annexin V/PE staining and flow cytometry assay. The line graph presents mean apoptotic rate. Data are presented as the mean ± SD of three independent experiments. $^{*}P<0.05$, $^{**}P<0.01$ and $^{***}P<0.001$. ITIH3, inter-α-trypsin inhibitor heavy chain 3; DDP, cisplatin; IC_{50}, half-maximal inhibitory concentration; RNAi, RNA interference; NC, negative control.
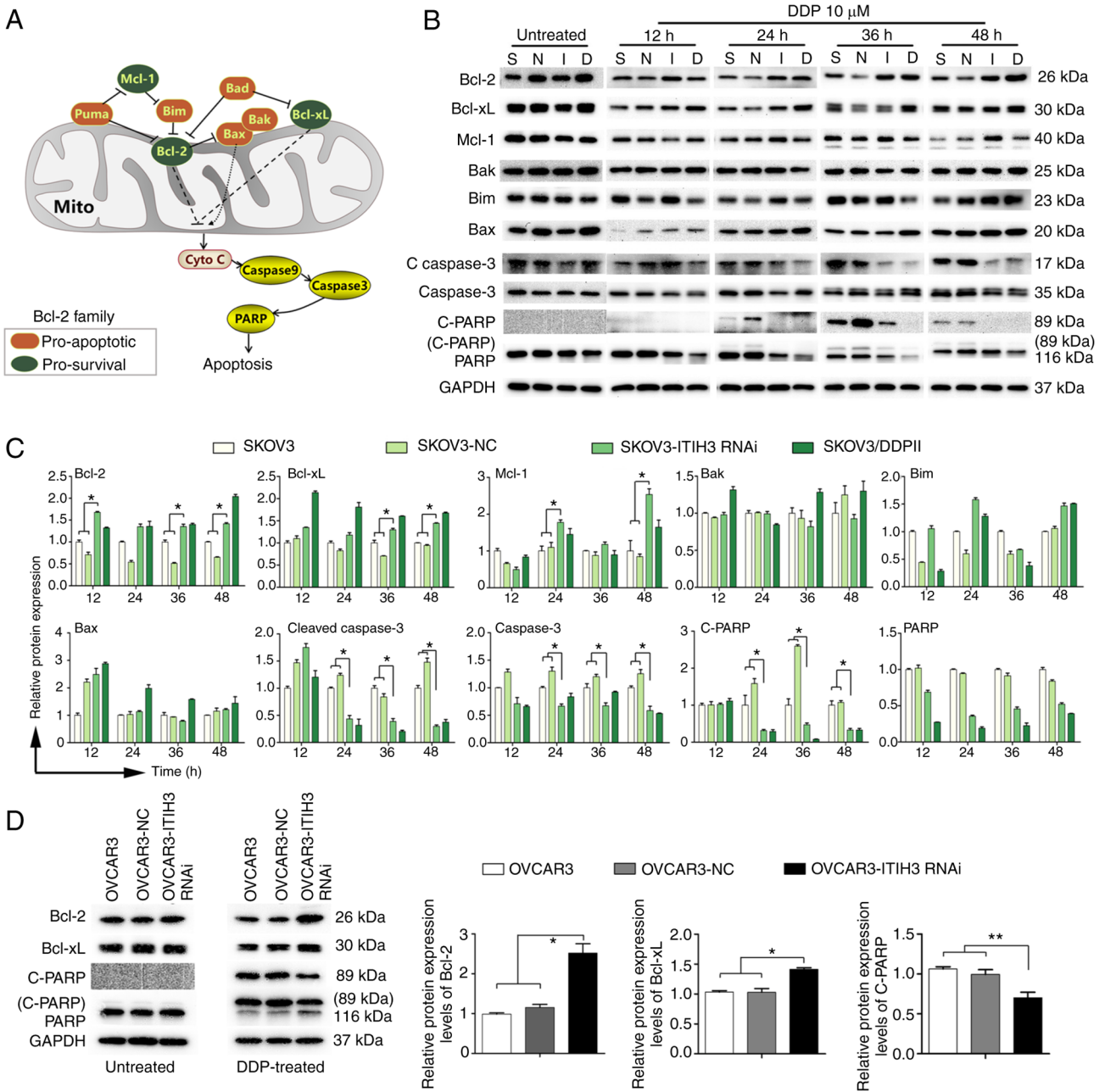
Figure 3. ITIH3 promotes Bcl-2 signaling *in vitro*. (A) Overview of the Bcl-2 signaling pathway. (B) Western blotting of Bcl-2, Bcl-xL, Mcl-1, Bak, Bim, Bax, C-Caspase 3, Caspase 3, C-PARP and PARP protein expression levels in SKOV3-NC, SKOV3-ITIH3 RNAi, SKOV3 and SKOV3/DDPII cells following treatment with 10 μM DDP for 12, 24, 36 and 48 h. (C) Bcl-2, Bcl-xL, Mcl-1, Bak, Bim, Bax, C-Caspase 3, Caspase 3 and C-PARP protein expression levels in SKOV3-NC, SKOV3-ITIH3 RNAi, Skov3 and SKOV3/DDPII cells following treatment with 10 μM DDP for 12, 24, 36 and 48 h. (D) Western blotting of Bcl-2, Bcl-xL, C-PARP and PARP protein expression levels in OVCAR3, OVCAR3-NC and OVCAR3-ITIH3 RNAi cells following treatment with 10 μM DDP for 36 h. GAPDH was used as a loading control. Data are presented as the mean ± SD of three independent experiments. *P<0.05 and **P<0.01. C, cleaved; Casp, caspase; RNAi, RNA interference; S, SKOV3; N, SKOV3-NC; I, SKOV3-ITIH3 RNAi; D, SKOV3/DDPII; ITIH3, inter-α-trypsin inhibitor heavy chain 3; DDP, cisplatin; NC, negative control; Mito, mitochondria.

levels of the pro-survival proteins Bcl-2, Bcl-xL and Mcl-1 in SKOV3-ITIH3 RNAi cells were markedly higher than in SKOV3 and SKOV3-NC cells (Fig. 3B). However, no marked difference in expression levels of pro-apoptotic proteins Bak, Bim and Bax was observed. The expression levels of the apoptotic proteins cleaved caspase 3 and caspase 3 and the cleaved DNA repair enzyme, C-PARP, were markedly decreased in SKOV3-ITIH3 RNAi cells compared with in SKOV3 and SKOV3-NC cells. Following DDP treatment for 12 h, Bcl-2 protein expression levels in SKOV3-ITIH3 RNAi cells were

significantly higher than those in SKOV3 and SKOV3-NC cells and similar to protein expression levels demonstrated in SKOV3/DDPII cells (Fig. 3C). Furthermore, 24 h after DDP treatment, Mcl-1 protein expression levels in SKOV3-ITIH3 RNAi cells were significantly higher and the protein expression of cleaved caspase 3 and caspase 3 were significantly decreased compared with those in SKOV3 and SKOV3-NC cells. C-PARP protein expression levels were significantly higher in SKOV3 and SKOV3-NC cells than those in SKOV3-ITIH3 RNAi. Following 10 μM DDP treatment for 36 h, Bcl-2 and
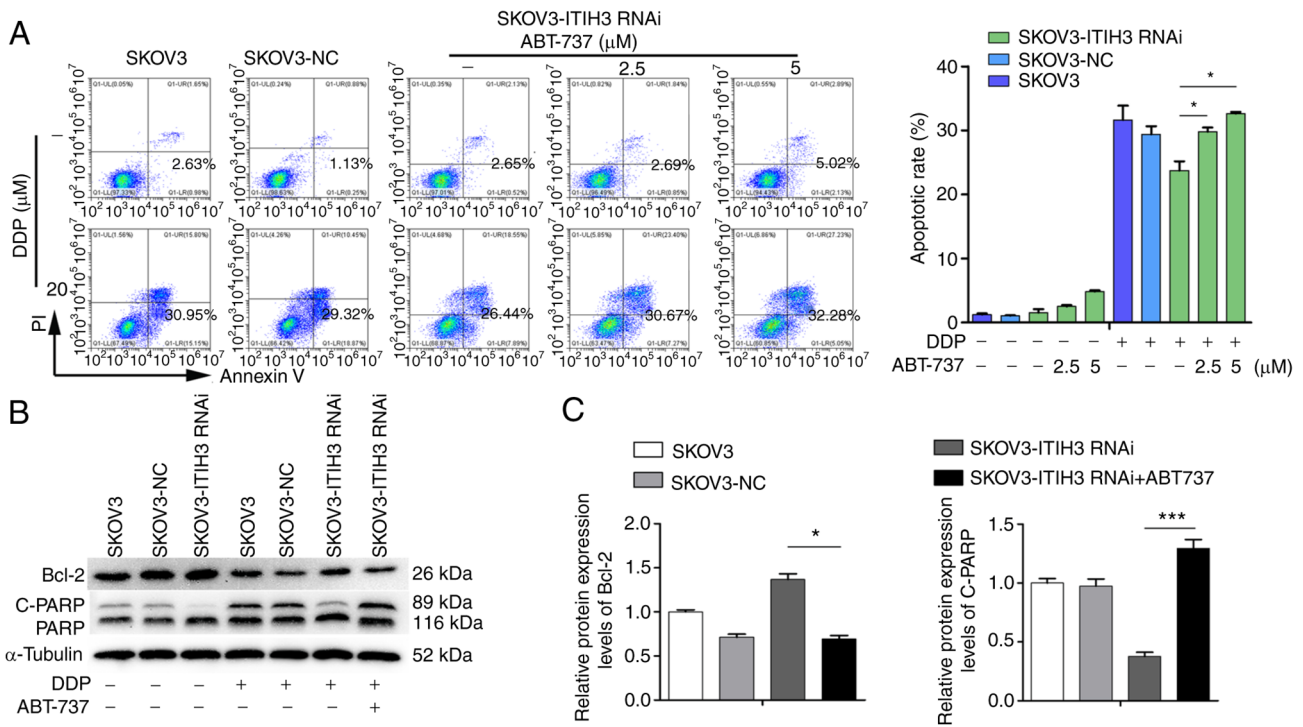
Figure 4. ITIH3-induced Bcl-2 signaling is reversed by Bcl-2 inhibitor ABT-737. (A) SKOV3-ITIH3 RNAi cells were treated with or without DDP (20 μM) and Bcl-2 inhibitor ABT-737 (2.5 and 5.0 μM) for 48 h. Apoptotic cell death was assessed using Annexin V/PE staining and flow cytometry assays. Histograms present the mean apoptotic rate. (B) Western blotting results of Bcl-2, PARP and C-PARP protein expression levels in SKOV3, SKOV3-NC and SKOV3-ITIH3 RNAi cells after treatment with or without DDP (10 μM) and ABT-737 (2.5 μM) for 48 h. Tubulin was used as a loading control. (C) Bcl-2 and C-PARP protein expression levels in SKOV3, SKOV3-NC and SKOV3-ITIH3 RNAi cells following treatment with DDP (10 μM) and ABT-737 (2.5 μM) for 48 h. Data are presented as the mean ± SD of three independent experiments. *P<0.05 and ***P<0.001. C, cleaved; Casp, caspase; RNAi, RNA interference; ITIH3, inter-α-trypsin inhibitor heavy chain 3; DDP, cisplatin; NC, negative control.

Bcl-xL protein expression levels in SKOV3-ITIH3 RNAi cells were significantly higher than in SKOV3 and SKOV3-NC cells; however, protein expression levels of cleaved caspase 3 and caspase 3 and C-PARP were significantly decreased. Following DDP treatment for 48 h, the protein expression levels of Bcl-2, Bcl-xL and Mcl-1 in SKOV3-ITIH3 RNAi cells were significantly higher than those in SKOV3 and SKOV3-NC cells, whereas cleaved caspase 3 and caspase 3 protein expression levels were significantly lower. C-PARP protein expression levels were almost undetectable in SKOV3-ITIH3 RNAi cells. These results indicated that following ITIH3 silencing, the inhibitory Bcl-2 signaling pathway in SKOV3 cells was significantly activated following DDP treatment and similar findings were demonstrated in SKOV3/DDPII cells *in vitro*.

To assess whether ITIH3 silencing regulates Bcl-2 signaling in other OC cells, Bcl-2, Bcl-xL, C-PARP and PARP protein expression levels were evaluated before and after DDP treatment using western blotting. The results demonstrated that before DDP treatment, the proteins demonstrated no marked difference in OVCAR3, OVCAR3-NC and OVCAR3-ITIH3 RNAi cells (Fig. 3D). Following 10 μM DDP treatment for 36 h, Bcl-2 and Bcl-xL protein expression levels in OVCAR3-ITIH3 RNAi cells were significantly higher than those in OVCAR3 and OVCAR3-NC cells (Fig. 3D), whereas C-PARP protein expression levels were significantly lower (Fig. 3D). These results indicated that following ITIH3 silencing, the inhibitory Bcl-2 pathway in OVCAR3 cells was significantly activated by DDP treatment.

Bcl-2 inhibitor ABT-737 reverses DDP resistance induced by ITIH3. The proportion of apoptotic cells in the SKOV3-ITIH3 RNAi cell line was not significantly increased following treatment with 2.5 μM ABT-737 for 48 h but was markedly increased after treatment with 5 μM ABT-737 compared with the untreated SKOV3-ITIH3 RNAi cells (Fig. 4A). However, the proportion of apoptotic SKOV3-ITIH3 RNAi cells following DDP (20 μM) and ABT-737 (2.5 and 5 μM) co-treatment for 48 h was significantly higher than with DDP alone for 48 h, which was similar to that of control SKOV3 and SKOV3-NC cells (Fig. 4A). Compared with treated DDP (10 μM) alone for 48 h, the protein expression levels of Bcl-2 in the SKOV3-ITIH3 RNAi cell line cotreated with DDP (10 μM) and ABT-737 (2.5 μM) were significantly decreased (Fig. 4B and C) and C-PARP protein expression levels were significantly increased, with similar protein expression levels to SKOV3 and SKOV3-NC cells.

ITIH3 may be an upstream regulator of the Bcl-2 family that promotes apoptosis induced by DDP in vivo. To evaluate the Bcl-2 induced apoptosis mechanisms, a subcutaneous murine xenograft model of SKOV3-ITIH3 RNAi cells and SKOV3-NC cells treated with DDP was established (Fig. 5A). *In vivo* experiments demonstrated that ITIH3 silencing enhanced DDP resistance in the xenograft nude mouse models; tumor volumes of the SKOV3-ITIH3 RNAi group were significantly higher than in the SKOV3-NC group following 5 and 8 DDP injections (Fig. 5B and C). Western blotting of xenograft
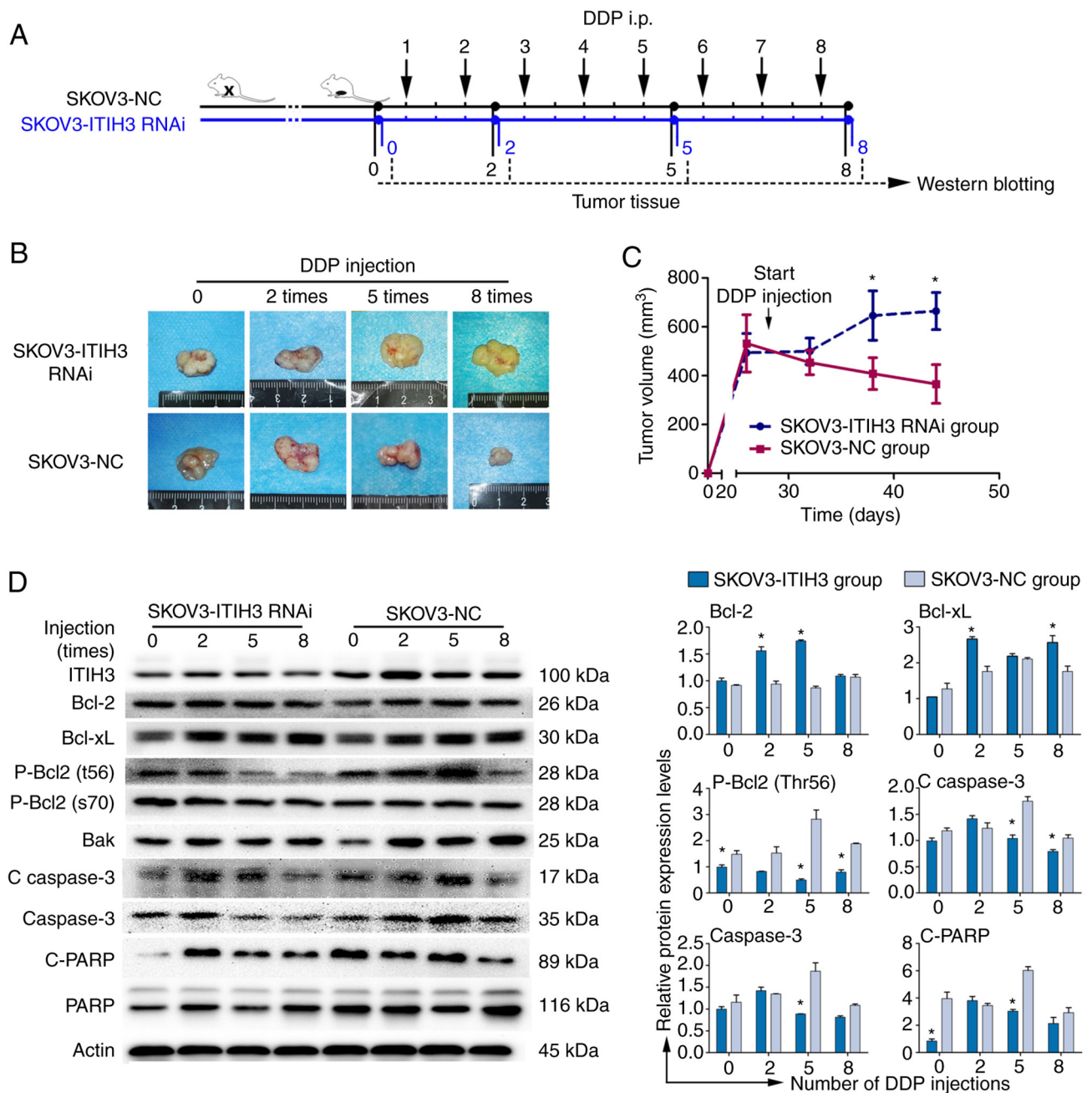
Figure 5. ITIH3 promotes Bcl-2 signaling *in vivo*. (A) Overview of the workflow in the mouse study. (B) Representative examples of SKOV3-ITIH3 RNAi- and SKOV3-NC-derived subcutaneous allograft tumors after 0, 2, 5 and 8 intraperitoneal DDP injections. (C) Tumor volumes were recorded from the date of injection to the end of the study (n=5/group). (D) Western blotting of ITIH3, Bcl-2, Bcl-xL, p-Bcl-2 (Thr56), p-Bcl-2 (ser70), Bak, cleaved caspase 3, caspase 3, C-PARP and PARP protein expression levels in SKOV3-NC, SKOV3-ITIH3 RNAi, SKOV3 and SKOV3/DDPII subcutaneous allograft tumor cells following 0, 2, 5 and 8 intraperitoneal DDP injections. GAPDH was used as a loading control. Data are presented as the mean ± standard deviation of three independent experiments. *P<0.05, vs. SKOV3-NC group. C, cleaved; RNAi, RNA interference; ITIH3, inter-α-trypsin inhibitor heavy chain 3; DDP, cisplatin; NC, negative control.

tumor proteins in nude mice demonstrated that protein expression levels in the SKOV3-ITIH3 RNAi group were similar to the SKOV3/DDPII group under the treatment of DDP. The expression levels of the pro-survival Bcl-2 and Bcl-xL proteins in the SKOV3-ITIH3 RNAi group were significantly increased following 2, 5 and 8 DDP injections compared with in SKOV3-NC group (Fig. 5D). P-Bcl-2 (Thr56) protein in the SKOV3-ITIH3 RNAi group was significantly decreased following 0, 5 and 8 DDP injections compared with in SKOV3-NC group (Fig. 5D). These results were substantiated

by the altered expression levels of downstream proteins. The protein expression levels of C-caspase 3, caspase 3 and C-PARP in the SKOV3-ITIH3 RNAi group were significantly lower than those in the SKOV3-NC group (Fig. 5D).

Discussion

At present, platinum-based chemotherapy combined with paclitaxel administration is the first-line chemotherapy regimen for OC (3). DDP resistance in OC cells is the

primary reason for the failure of chemotherapy treatment (4). Therefore, it is necessary to understand the molecules that regulate chemoresistance and to evaluate novel methods to circumvent multidrug resistance. iTRAQ proteomic profiling in the SKOV3 and SKOV3/DDPII xenograft models demonstrated that with an increase in the number of DDP injections, ITIH3 protein expression levels in mice injected with drug-resistant SKOV3/DDPII cells was markedly lower than in the control group, which was consistent with western blotting results. These results indicated that ITIH3 may be involved in the increased sensitivity of OC cells to chemotherapy. Subsequently, the association between ITIH3 protein expression levels and prognosis was assessed in tumor tissue from patients with OC. The results demonstrated that the OS of the high ITIH3 protein expression level group was significantly higher than the low ITIH3 protein expression group. Furthermore, in a preliminary study (5,23), the association between ITIH3 protein expression levels and key Bcl-2 signaling pathway proteins, as well as the OS of patients with high and low protein expression levels of Bcl-2 in OC were assessed using The Cancer Genome Atlas database (24). The results demonstrated that the protein expression levels of Bcl-2 were not significantly associated with to prognosis in OC tissues without chemotherapy (data not shown), therefore the Bcl-2 protein expression of TMAs was not assessed in the present study. The results of the present study indicated that loss of ITIH3 protein expression was associated with poor prognosis in patients with late-stage OC.

An increasing number of studies have reported that ITIH3 protein expression levels are abnormally elevated in the blood of patients with various tumors, such as pancreatic, early gastric and colorectal cancer, and may serve as a new tumor marker (9-13). Moreover, several studies have reported that the ITIH3 gene is significantly downregulated in numerous human solid tumors (8,25). ITIH3 mRNA is reported to be highly expressed in healthy ovaries but downregulated in 71% of OC cases, which indicates that ITIH3 may be an OC suppressor gene (8). The function of the ITIH3 gene and its role in the development of OC is not fully known. In the present study, ITIH3 silencing significantly increased SKOV3 cell resistance to DDP and increased DDP-mediated colony formation of SKOV3 cells. Furthermore, ITIH3 silencing significantly decreased DDP-induced apoptosis of SKOV3 cells. These results suggested that ITIH3 may be a key upstream molecule for the regulation of platinum resistance in OC.

The most common mechanism of tumor cell death in platinum-based chemotherapy is apoptosis (26), programmed cell death process regulated by numerous signaling molecules (27). The Bcl-2 family has been reported to serve an important role in the mitochondrial apoptosis pathway (28,29). Bcl-2, Bcl-xL and Mcl-1 bind to the outer mitochondrial membrane and exert anti-apoptotic effects by inhibiting cytochrome C release and caspase activation (30). Pro-apoptotic proteins such as Bax, Bak and Bim primarily act on the outer mitochondrial membrane, where they form microporous channels to increase membrane permeability and cause cytochrome C release, which leads to apoptosis (30). In the present study, expression levels of Bcl-2 family proteins demonstrated no significant difference between ITIH3 RNAi cells and the control cells before DDP treatment. However, protein expression levels of Bcl-2 family anti-apoptotic Bcl-2, Bcl-xL and Mcl-1 were significantly upregulated in ITIH3 RNAi cells compared with control cells following treatment with the same concentration of DDP. Furthermore, after DDP treatment, there was no significant change in expression levels of Bcl-2 family pro-apoptotic proteins such as Bak and Bax, whereas expression levels of downstream apoptosis proteins cleaved caspase3, caspase 3 and C-PARP were significantly downregulated in ITIH3 RNAi cells. The Bcl-2 inhibitor ABT-737 significantly reversed the decreased apoptotic rate in SKOV3 cells induced by silencing ITIH3. Moreover, ABT-737 induced downregulation of Bcl-2 expression and upregulated C-PARP expression in SKOV3-ITIH3 RNAi cells. Taken together, these results indicated that ITIH3 was involved in the development of the resistance of cancer cells to DDP treatment by regulating both pro- and anti-apoptotic Bcl-2 family member-dependent pathways.

The common phosphorylation sites of Bcl-2 are Ser70, Ser87, Thr74 and Thr56 (31). A previous study reported that dephosphorylation, even at a single site, significantly increases resistance to apoptosis (32). When cells are exposed to drugs, Bcl-2 is usually phosphorylated to decrease or even lose its anti-apoptotic ability, which leads to apoptosis (32,33). The *in vivo* animal experiments of the present study demonstrated that with an increased number of DDP doses, Bcl-2 and Bcl-xL protein expression levels in the SKOV3-ITIH3 RNAi group markedly increased and phosphorylated Bcl-2 (Thr56) protein expression levels decreased. This result indicated that the anti-apoptotic ability of the SKOV3-ITIH3 RNAi group was higher than the control group, which was substantiated by changes in downstream caspase and C-PARP protein expression levels. Moreover, both *in vivo* and *in vitro* experiments demonstrated that following ITIH3 silencing, expression levels of proteins in the Bcl-2 signaling pathway, especially anti-apoptotic proteins, markedly increased, which led to enhanced tumor cell resistance to DDP. Moreover, silencing of ITIH3 could attenuate DDP-induced apoptosis via the Bcl-2 signaling pathway.

ITIH3 is one of five heavy chain proteins (ITIH1, ITIH2, ITIH3, ITIH4 and ITIH5) that comprise the intertype trypsin inhibitor family and can covalently bind hyaluronic acid (34). ITIH3 has been reported to be associated with various solid tumors and diseases, as well as mental health conditions (35,36), rheumatoid arthritis (37) and sepsis (15), which indicates its potential research value. It was hypothesized that ITIH3 expression was associated with activation of platinum sensitivity in OC. The *in vivo* and *in vitro* experiments of the present study demonstrated that ITIH3 participated in controlling the sensitivity of OC cells to DDP via regulation of the Bcl-2 signaling pathway and that Bcl-2 inhibitors reversed this phenomenon. However, the specific regulatory mechanism remains unclear. The ITI protein family is widely hypothesized to serve a key role in extracellular matrix biology (38-40). Our previous study demonstrated that intracellular DDP accumulation in SKOV3 cells was 6.4-fold higher than in SKOV3/DDPII cells following addition of DDP (5). Overall, the results of the present study suggested that ITIH3 may affect the concentration of platinum drugs in these cells. The study presents some limitations. The first is only one DDP-resistance cell line was tested in this study. The second limitation is the lack of

ITIH3 overexpression experiments in DDP-resistance cell line. Nonetheless, further studies in *de novo* resistant cell lines or DDP resistance tumor tissues are required to support the results of the present study.

To the best of our knowledge, this is the first study to demonstrated the association between ITIH3 downregulation in tumor cells and enhanced drug resistance *in vivo* and *in vitro*. Following ITIH3 silencing, expression levels of proteins in the Bcl-2 signaling pathway, especially anti-apoptotic proteins, markedly increased, which led to increased drug resistance in tumor cells. Therefore, the results of the present study indicated that ITIH3 was a potential biomarker of DDP resistance in OC.

Acknowledgements

Funding

Availability of data and materials

The datasets used and/or analyzed during the current study are available from the corresponding author on reasonable request.

Authors' contributions

Conceptualization was performed by QW, DY and YF. Research methods were carried out by QW, DY, CY, YL, LS, ML, HL and XC. Data analysis was performed by YL, LS, CY, YF and XC. YL wrote the original draft of the manuscript. Funding was acquired by QW and CY. All authors have read and approved the final manuscript. YL, LS and QW confirm the authenticity of all the raw data.

Ethics approval and consent to participate

The study involving human participants was approved by The Scientific Ethics Committee of Qilu Hospital of Shandong University (approval no. KYLL-2013-130). All participants provided written informed consent for this study. All procedures were performed in accordance with relevant guidelines and regulations. All animal experiments were approved by the Animal Ethics Committee of Guangxi Medical University Affiliated Tumor Hospital (approval no. 2021057). The animal study was performed in compliance with the Animal Research:

Reporting of *In Vivo* Experiments guidelines and all methods were performed in accordance with relevant guidelines and regulations.

Patient consent for publication

Not applicable.

Competing interests

The authors declare that they have no competing interests.

References

1. Siegel RL, Miller KD and Jemal A: Cancer statistics, 2020. CA Cancer J Clin 70: 7-30, 2020.
2. Rottenberg S, Disler C and Perego P: The rediscovery of platinum-based cancer therapy. Nat Rev Cancer 21: 37-50, 2021.
3. Kuroki L and Guntupalli SR: Treatment of epithelial ovarian cancer. BMJ 371: m3773, 2020.
4. Matulonis UA, Sood AK, Fallowfield L, Howitt BE, Sehouli J and Karlan BY: Ovarian cancer. Nat Rev Dis Primers 2: 16061, 2016.
5. Shi L, Yu H, Zhang W, Li L and Wang Q: Establishment and biological characteristics of a platinum-resistance nude mouse model in epithelial ovarian cancer. Zhonghua Fu Chan Ke Za Zhi 49: 523-530, 2014 (In Chinese).
6. Bost F, Diarra-Mehrpour M and Martin JP: Inter-alpha-trypsin inhibitor proteoglycan family-a group of proteins binding and stabilizing the extracellular matrix. Eur J Biochem 252: 339-346, 1998.
7. Zhuo L, Hascall VC and Kimata K: Inter-alpha-trypsin inhibitor, a covalent protein-glycosaminoglycan-protein complex. J Biol Chem 279: 38079-38082, 2004.
8. Hamm A, Veeck J, Bektas N, Wild PJ, Hartmann A, Heindrichs U, Kristiansen G, Werbowetski-Ogilvie T, Del Maestro R, Knuechel R and Dahl E: Frequent expression loss of Inter-alpha-trypsin inhibitor heavy chain (ITIH) genes in multiple human solid tumors: A systematic expression analysis. BMC Cancer 8: 25, 2008.
9. Kopylov AT, Stepanov AA, Malsagova KA, Soni D, Kushlinsky NE, Enikeev DV, Potoldykova NV, Lisitsa AV and Kaysheva AL: Revelation of proteomic indicators for colorectal cancer in initial stages of development. Molecules 25: 619, 2020.
10. Liu X, Zheng W, Wang W, Shen H, Liu L, Lou W, Wang X and Yang P: A new panel of pancreatic cancer biomarkers discovered using a mass spectrometry-based pipeline. Br J Cancer 118: e15, 2018.
11. Peng H, Pan S, Yan Y, Brand RE, Petersen GM, Chari ST, Lai LA, Eng JK, Brentnall TA and Chen R: Systemic proteome alterations linked to early stage pancreatic cancer in diabetic patients. Cancers (Basel) 12: 1534, 2020.
12. Chong PK, Lee H, Zhou J, Liu SC, Loh MC, Wang TT, Chan SP, Smoot DT, Ashktorab H, So JB, *et al*: ITIH3 is a potential biomarker for early detection of gastric cancer. J Proteome Res 9: 3671-3679, 2010.
13. Dufresne J, Bowden P, Thavarajah T, Florentinus-Mefailoski A, Chen ZZ, Tucholska M, Norzin T, Ho MT, Phan M, Mohamed N, *et al*: The plasma peptides of breast versus ovarian cancer. Clin Proteomics 16: 43, 2019.
14. Ivancic MM, Huttlin EL, Chen X, Pleiman JK, Irving AA, Hegeman AD, Dove WF and Sussman MR: Candidate serum biomarkers for early intestinal cancer using 15N metabolic labeling and quantitative proteomics in the ApcMin/+ mouse. J Proteome Res 12: 4152-4166, 2013.
15. Thavarajah T, Dos Santos CC, Slutsky AS, Marshall JC, Bowden P, Romaschin A and Marshall JG: The plasma peptides of sepsis. Clin Proteomics 17: 26, 2020.
16. Feng Y, Tang Y, Mao Y, Liu Y, Yao D, Yang L, Garson K, Vanderhyden BC and Wang Q: PAX2 promotes epithelial ovarian cancer progression involving fatty acid metabolic reprogramming. Int J Oncol 56: 697-708, 2020.
17. Dongol S, Zhang Q, Qiu C, Sun C, Zhang Z, Wu H and Kong B: IQGAP3 promotes cancer proliferation and metastasis in high-grade serous ovarian cancer. Oncol Lett 20: 1179-1192, 2020.

18. Wu H, Li R, Zhang Z, Jiang H, Ma H, Yuan C, Sun C, Li Y and Kong B: Kallistatin inhibits tumour progression and platinum resistance in high-grade serous ovarian cancer. J Ovarian Res 12: 125, 2019.
19. Meng Q, Duan P, Li L and Miao Y: Expression of placenta growth factor is associated with unfavorable prognosis of advanced-stage serous ovarian cancer. Tohoku J Exp Med 244: 291-296, 2018.
20. Zhang R, Hao J, Wu Q, Guo K, Wang C, Zhang WK, Liu W, Wang Q and Yang X: Dehydrocostus lactone inhibits cell proliferation and induces apoptosis by PI3K/Akt/Bad and ERS signalling pathway in human laryngeal carcinoma. J Cell Mol Med 24: 6028-6042, 2020.
21. Wang Q, Tang Y, Yu H, Yin Q, Li M, Shi L, Zhang W, Li D and Li L: CCL18 from tumor-cells promotes epithelial ovarian cancer metastasis via mTOR signaling pathway. Mol Carcinog 55: 1688-1699, 2016.
22. Kilkenny C, Browne WJ, Cuthill IC, Emerson M and Altman DG: Improving bioscience research reporting: The ARRIVE guidelines for reporting animal research. PLoS Biol 8: e1000412, 2010.
23. Chen F, Sun F, Liu X, Shao J and Zhang B: Glaucocalyxin A inhibits the malignant progression of epithelial ovarian cancer by affecting the MicroRNA-374b-5p/HMGB3/Wnt-β-catenin pathway axis. Front Oncol 12: 955830, 2022.
24. Wang Z, Jensen MA and Zenklusen JC: A Practical guide to the cancer genome atlas (TCGA). Methods Mol Biol 1418: 111-141, 2016.
25. Jiang X, Bai XY, Li B, Li Y, Xia K, Wang M, Li S and Wu H: Plasma inter-alpha-trypsin inhibitor heavy chains H3 and H4 serve as novel diagnostic biomarkers in human colorectal cancer. Dis Markers 2019: 5069614, 2019.
26. Wijdeven RH, Pang B, Assaraf YG and Neefjes J: Old drugs, novel ways out: Drug resistance toward cytotoxic chemotherapeutics. Drug Resist Updat 28: 65-81, 2016.
27. Wlodkowic D, Telford W, Skommer J and Darzynkiewicz Z: Apoptosis and beyond: Cytometry in studies of programmed cell death. Methods Cell Biol 103: 55-98, 2011.
28. Martinou JC and Youle RJ: Mitochondria in apoptosis: Bcl-2 family members and mitochondrial dynamics. Dev Cell 21: 92-101, 2011.
29. Youle RJ and Strasser A: The BCL-2 protein family: Opposing activities that mediate cell death. Nat Rev Mol Cell Biol 9: 47-59, 2008.
30. Singh R, Letai A and Sarosiek K: Regulation of apoptosis in health and disease: The balancing act of BCL-2 family proteins. Nat Rev Mol Cell Biol 20: 175-193, 2019.
31. Maundrell K, Antonsson B, Magnenat E, Camps M, Muda M, Chabert C, Gillieron C, Boschert U, Vial-Knecht E, Martinou JC and Arkinstall S: Bcl-2 undergoes phosphorylation by c-Jun N-terminal kinase/stress-activated protein kinases in the presence of the constitutively active GTP-binding protein Rac1. J Biol Chem 272: 25238-25242, 1997.
32. Yamamoto K, Ichijo H and Korsmeyer SJ: BCL-2 is phosphorylated and inactivated by an ASK1/Jun N-terminal protein kinase pathway normally activated at G(2)/M. Mol Cell Biol 19: 8469-8478, 1999.
33. Huang ST and Cidlowski JA: Phosphorylation status modulates Bcl-2 function during glucocorticoid-induced apoptosis in T lymphocytes. FASEB J 16: 825-832, 2002.
34. Ebana Y, Ozaki K, Inoue K, Sato H, Iida A, Lwin H, Saito S, Mizuno H, Takahashi A, Nakamura T, et al: A functional SNP in ITIH3 is associated with susceptibility to myocardial infarction. J Hum Genet 52: 220-229, 2007.
35. Xie X, Meng H, Wu H, Hou F, Chen Y, Zhou Y, Xue Q, Zhang J, Gong J, Li L and Song R: Integrative analyses indicate an association between ITIH3 polymorphisms with autism spectrum disorder. Sci Rep 10: 5223, 2020.
36. Li K, Li Y, Wang J, Huo Y, Huang D, Li S, Liu J, Li X, Liu R, Chen X, et al: A functional missense variant in ITIH3 affects protein expression and neurodevelopment and confers schizophrenia risk in the Han Chinese population. J Genet Genomics 47: 233-248, 2020.
37. Liao CC, Chou PL, Cheng CW, Chang YS, Chi WM, Tsai KL, Chen WJ, Kung TS, Tai CC, Lee KW, et al: Comparative analysis of novel autoantibody isotypes against citrullinated-inter-alpha-trypsin inhibitor heavy chain 3 (ITIH3)(542-556) peptide in serum from Taiwanese females with rheumatoid arthritis, primary Sjögren's syndrome and secondary Sjögren's syndrome in rheumatoid arthritis. J Proteomics 141: 1-11, 2016.
38. Cuvelier A, Muir JF, Martin JP and Sesboüé R: Proteins of the inter-alpha trypsin inhibitor (ITI) family. A major role in the biology of the extracellular matrix. Rev Mal Respir 17: 437-446, 2000 (In French).
39. Zhuo L and Kimata K: Structure and function of inter-alpha-trypsin inhibitor heavy chains. Connect Tissue Res 49: 311-320, 2008.
40. Hennies HC: All is balanced: Inter-α-trypsin inhibitors as unseen extracellular matrix proteins in epidermal morphology and differentiation. Exp Dermatol 24: 661-662, 2015.